Convection in rotating annuli: Ginzburg-Landau equations with tunable coefficients

Martin van Hecke* and Wim van Saarloos
Instituut-Lorentz, Leiden University, P.O. Box 9506, 2300 RA Leiden, The Netherlands
(Received 13 September 1996)

The coefficients of the complex Ginzburg-Landau equations that describe weakly nonlinear convection in a large rotating annulus are calculated for a range of Prandtl numbers σ. For fluids with $\sigma \approx 0.15$, we show that the rotation rate can tune the coefficients of the corresponding amplitude equations from regimes where coherent patterns prevail to regimes of spatiotemporal chaos. [S1063-651X(97)50701-X]

PACS number(s): 47.20.Bp, 47.20.Ky, 03.40.Gc, 47.32.−y

The complex Ginzburg-Landau equation (CGLE)

$$\partial_t A = A + (1+ic_1)\partial_x^2 A - (1-ic_3)|A|^2 A, \qquad (1)$$

which describes slow modulations of an amplitude or envelope A near a Hopf bifurcation in spatially extended systems, has been used extensively both to study nonequilibrium pattern formation [1,2] and as a model system for spatiotemporal chaos [3,4]. The qualitative dynamical behavior of solutions of the CGLE depends on the coefficients c_1 and c_3, which, for a given system, can be obtained from the underlying equations by laborious calculations (see e.g., [5] for binary mixture convection). For c_1 and c_3 small, as well as close to the line $c_3 = -c_1$, the dynamics is close to that found in the relaxational limit $c_1 = c_3 = 0$, whereas for $|c_1|$ and $|c_3|$ large, the CGLE reduces to the nonlinear Schrödinger equation. In recent years, the complicated and often surprising dynamics that occurs away from these limits, has been intensively studied theoretically [3,4]. In particular, it has become clear that the CGLE shows various regimes of spatiotemporal chaos when $c_1 c_3 > 1$; see Fig. 1. The precise nature of the various chaotic regimes, as well as the existence and nature of the transitions between them, is still under active investigation in the field of spatiotemporal chaos.

In order to be able to investigate these chaotic regimes *experimentally*, one would like to have a system where the coefficients of the corresponding CGLE can be tuned in a convenient way through the spatiotemporal chaotic regimes. So far, only one experiment appears to be known where there is indirect evidence that these regimes are accessed [6,7]. When it was discovered that a forward Hopf bifurcation to a quasi-one-dimensional wall-mode occurs in rotating Rayleigh-Bénard convection in bounded containers [8], it was realized that the rotation rate might serve to tune the coefficients of the corresponding CGLE [9]. Kuo and Cross therefore performed the amplitude expansion for such a rotating cylinder of infinite radius and $\sigma = 6.4$ (corresponding to water), but, unfortunately, found that the coefficients remain close to the relaxational line $c_1 = -c_3$ for arbitrary values of the rotation rate Ω [10]. Our results for the annulus, illustrated by the heavy line for $\sigma = 6.7$ in Fig. 1, confirm this for essentially all Prandtl numbers larger than 0.2.

In order to obtain an experimental realization of the CGLE with coefficients that can be tuned by the rotation rate over a much wider range, we have investigated convection in rotating annuli for a range of Prandtl numbers. We take the circumference of the annulus large enough that the curvature can be neglected. This geometry differs from a cylindrical one in that bulk-modes are quasi-one-dimensional and can be described by the same amplitude equations as the wall-modes, and that there are *two* wall-modes, localized near both side-walls. The infinite radius limit allows the use of Euclidean instead of cylindrical coordinates and circumvents the wavenumber discretization that occurs in a finite con-

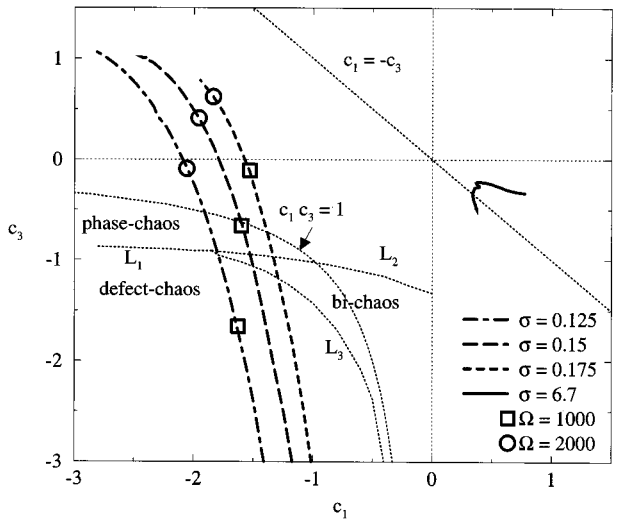

FIG. 1. Part of the phase diagram of the CGLE. Since the CGLE is invariant under $c_1 \to -c_1$, $c_3 \to -c_3$, so is the phase diagram. The diagonal line $c_1 = -c_3$ indicates the relaxational limit of the CGLE, while the curve $c_1 c_3 = 1$ corresponds to the Newell criterion [1]; outside of this hyperbola chaos occurs. The various spatiotemporal chaotic regimes and the lines L_1, L_2, and L_3 separating them [3,4] are indicated, and the thick lines denote the results of our calculations. For $\sigma = 6.7$, the coefficients stay close to the relaxational limit, similar to [10], but for σ around 0.15 the rotation rate is able to tune c_1 and c_3 from close to the relaxational limit to deep into the spatiotemporal chaotic regime. The variation with the dimensionless rotation rate Ω is illustrated by the datapoints for $\Omega = 1000$ and $\Omega = 2000$.

*Present address: Center for Chaos and Turbulence Studies, The Niels Bohr Institute, Blegdamsvej 17, 2100 Copenhagen Ø, Denmark.

tainer [10,11]. In a system of finite radius, the two wall-modes will differ slightly, and as a result modes that are stationary in the infinite radius system acquire a small frequency [12]; we will ignore these effects. The main result of our calculations, illustrated in Fig. 1, is that for $0.1 \lesssim \sigma \lesssim 0.2$ traveling waves in a rotating annulus are predicted to be an experimental realization of a CGLE whose coefficients scan through the spatiotemporal chaotic part of the phase diagram when the rotation rate is changed.

The relevant mode in the interesting low Prandtl number regime is, however, not the analog of the wall-mode [8,10]. We have found that the σ dependence of the wall mode is weak, and its coefficients remain close to the relaxational limit. However, in an annulus of finite width, the oscillatory bulk mode identified already long ago for an infinite container [13,14], becomes the primary bifurcation from the nonconvective regime for a range of the rotation rates and $0.1 \lesssim \sigma \lesssim 0.2$. It is this bulk mode whose coefficients have the desired behavior. For even smaller values of σ, several nearby branches compete and no simple picture emerges [15].

Our calculations are based on standard methods to calculate the coefficients of the amplitude equations (see, e.g., [5]), but are complicated by computational difficulties and the occurrence of several competing branches of solutions for σ. Since a detailed account of the calculations and the results is given in [15], we confine our presentation here to a description of the basic setup and a summary of the most important predictions.

The amplitude equations describing the slow modulations of a right-traveling mode with (x,t) dependence $e^{i(-k_c x+\omega_c t)}$ and amplitude A, coupled to a left-traveling mode $e^{i(k_c x+\omega_c t)}$ with amplitude B, are [1,16]

$$\tau_0(\partial_t + v_g\partial_x)A = \varepsilon(1+ic_0)A + \xi_0^2(1+ic_1)\partial_x^2 A - g_0(1-ic_3)|A|^2A - g_2(1-ic_2)|B|^2A, \tag{2a}$$

$$\tau_0(\partial_t - v_g\partial_x)B = \varepsilon(1+ic_0)B + \xi_0^2(1+ic_1)\partial_x^2 B - g_0(1-ic_3)|B|^2B - g_2(1-ic_2)|A|^2B. \tag{2b}$$

For Rayleigh-Bénard convection, $\varepsilon := (R-R_c)/R_c$, with R the Rayleigh number $g\alpha\Delta T d^3/\kappa\nu$, where g is the gravitational acceleration, α the thermal expansion coefficient, ΔT the temperature difference between bottom and top plate, d the height of the layer, κ the thermal diffusivity, and ν the kinematic viscosity; R_c is the critical Rayleigh number. These quantities arise in the equations of motion that describe the fluid system in the corotating frame, which are the Navier-Stokes equation with additional centrifugal and Coriolis force, supplemented by the heat equation and the mass conservation law [13]. As usual [10,11,13,14], we apply the Boussinesq approximation and neglect the centrifugal forces.

Below we shall summarize our findings for all the coefficients and parameters in the amplitude equations. Since we find that $g_2 > g_0$ for the bulk mode, the standing waves are suppressed [1] and the relevant dynamical states are traveling wave states with, e.g., $A \neq 0$, $B = 0$. Upon rescaling time, space and the amplitude, Eq. (2a) then reduces to the CGLE (1) in the frame moving with the group velocity v_g.

As a length scale we choose d, so the top and bottom plates are at $z=0$ and $z=1$. We focus here on the case that the width of the channel is 1; for nearby values of the width similar behavior occurs, as detailed in [15]. The rotating (infinite radius) annulus is therefore characterized by two parameters. The first is the Prandtl number $\sigma := \nu/\kappa$. The second is the dimensionless rotation rate $\Omega := \Omega_D d^2/\nu$, where Ω_D is the angular velocity. In a typical experiment, σ is fixed, and the rotation rate Ω can be adjusted over a certain range up to values of order 10^4. To be able to separate the hydrodynamic equations, we assume slip boundary conditions on the top and bottom plates, as in [10]. On the vertical sidewalls we apply stick boundary conditions, which damp the mean flow that plays a role for low Prandtl number convection with slip boundary conditions [17]

$$v_x = v_y = v_z = \partial_y\theta = 0 \quad \text{on } y = 0,1, \tag{3a}$$

$$\partial_z v_x = \partial_z v_y = v_z = \theta = 0 \quad \text{on } z = 0,1, \tag{3b}$$

where θ is the deviation of the temperature from the conductive state profile. It should be noted that our version of the stick boundary conditions is slightly simpler than those used in [10]. We have normalized the amplitudes such that $|A|$ represents the ratio of convected to conducted heat; the value of g_0 therefore determines the so-called Nusselt number [10].

Bifurcation structure and linear stability. From the equations of motion we have determined R_c, which is the value of the Rayleigh number where convection sets in, and the corresponding critical wave number k_c and frequency ω_c as a function of σ and Ω. An important feature of our system is that there exists, in particular for small σ's, a multitude of solutions to the linearized equations, but only the mode with the *lowest* critical Rayleigh number is relevant. For a finite cylinder, these branches are discussed in detail in [11].

The relevant features of the bifurcation structure are illustrated in Fig. 2 and can be summarized as follows. (a) The linear stability analysis for the stationary modes is not dependent on the value of σ [15]. (b) For all $\sigma \gtrsim 0.2$, the wall-mode is relevant for sufficiently large rotation rates, while a stationary (nonoscillatory) mode is relevant for small Ω; see Fig. 2(c). For $\sigma = 6.7$ the crossover between the stationary and oscillatory modes occurs at $\Omega \approx 27.5$; the situation for $\sigma = 6.7$ is representative for the whole range $\sigma \gtrsim 0.2$. (c) The bulk-mode exists for values of σ that are comparable to where the Hopf bifurcation in an infinite layer occurs [13,14], and approaches this mode rapidly upon increasing the width of the annulus. (d) For $0.1 \lesssim \sigma \lesssim 0.2$ we find a band of rotation rates $\Omega_{min} < \Omega < \Omega_{max}$ for which the bulk-mode is *relevant*. See Fig. 2(c), where $\Omega_{min} = 140$ and $\Omega_{max} = 5600$ are marked. The situation for $\sigma = 0.15$ studied below is representative, as Fig. 2(d) for $\sigma = 0.175$ shows. (e) When $\sigma < 0.1$, the situation becomes quite convoluted since additional modes become relevant for some range of Ω's.

Amplitude expansion. The amount of computer time that is needed for the calculation of the nonlinear coefficients g_0, c_3, g_2, and c_2 of the coupled amplitude equations (2) is substantial; therefore, we cannot scan all system parameters

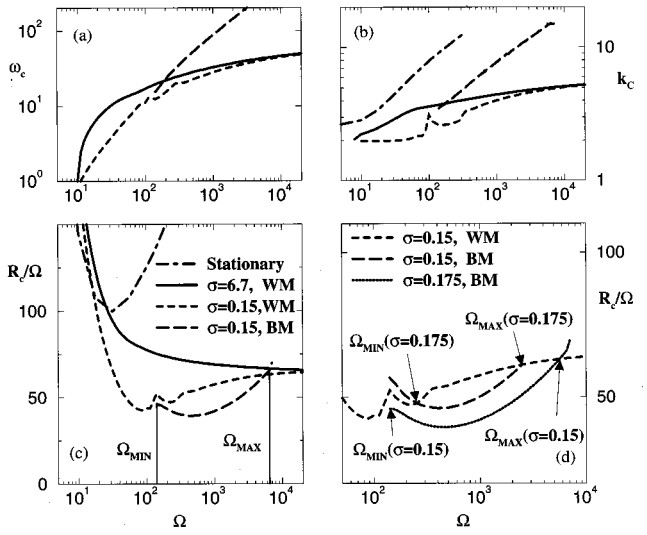

FIG. 2. (a)–(c) The linear onset values of bulk- (BM) and wall-modes (WM) as a function of Ω for $\sigma=6.7$ and 0.15. In (c) and (d) we have rescaled the critical Rayleigh numbers by Ω to facilitate the comparison between the various modes. The stationary bifurcation is seen to be the primary bifurcation for small rotation rates. For all $\sigma \gtrsim 0.2$, the wall-mode constitutes the primary mode for sufficiently large Ω as illustrated for the case $\sigma=6.7$. For $\sigma=0.15$, the bulk-mode exists for all $\Omega>\Omega_{min}\approx 140$. Its critical Rayleigh number is smaller than the critical Rayleigh number of the wall-mode for $\Omega_{min}<\Omega<\Omega_{max}\approx 5600$. It is in this range that the coefficients of the CGLE can be tuned over a wide range. In (a) and (b) the corresponding critical frequencies and wave numbers are plotted. (d) For values of the Prandtl number around 0.15, the critical Rayleigh numbers of the wall-mode only show a weak dependence on the Prandtl number, whereas those for the bulk-mode strongly depend on σ. As a result, the range of rotation rates for which the bulk-mode is relevant strongly depends on σ; for $\sigma=0.175$, the values of Ω_{min} and Ω_{max} are approximately 200 and 2500, while for $\sigma=0.125$ (not shown) they are 122 and 10 500.

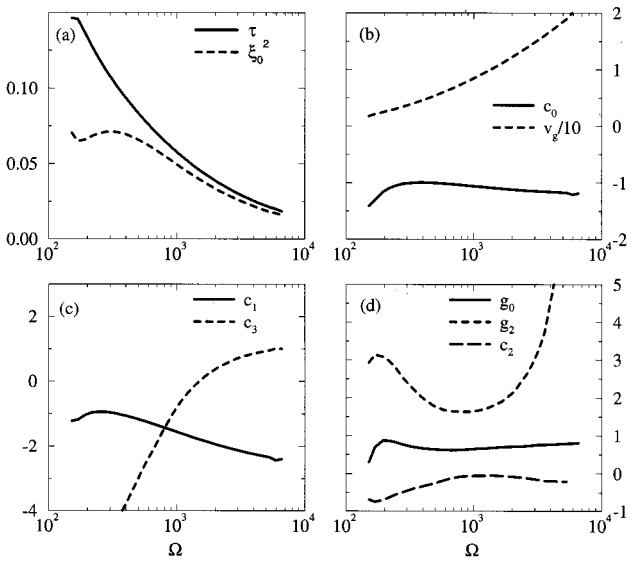

FIG. 3. The coefficients of Eq. (2) for the bulk-mode for $\sigma=0.15$. The coefficients c_1 and in particular c_3 have a strong dependence of the rotation rate (c). For $\Omega\to\Omega_{max}$, c_1 and c_3 are close to the relaxational limit. When the rotation rate is decreased c_3 changes sign, and at $\Omega\approx 1050$, the Newell criterion is reached ($c_1c_3=1$). A further decrease of the rotation rate pushes the coefficients deep into the spatio-temporal chaotic regime, as Fig. 1 shows.

simultaneously. Instead, we have performed a ''trial and error'' search in the (Ω,σ) space. We shall not exhaust the reader with the data thus obtained but concentrate on the wall- and bulk-mode discussed above and to a few values of σ that are representative for the various ranges of the Prandtl number. The dependence of the coefficients c_1 and c_3 of Eq. (2) for these two modes is illustrated in Figs. 1 and 3.

For the wall-modes, we find that the precise value of σ is quite irrelevant; the coefficients c_1 and c_3 of the amplitude equations are always near the $c_1=-c_3$ line, as the full line in Fig. 1 shows for $\sigma=6.7$. When Ω is sufficiently large, the wall-modes at the opposite sides of the boundary are decoupled and we recover the result of Kuo and Cross [10]. Of course, we have performed extensive searches in parameter space to search for more interesting behavior of the coefficients c_1 and c_3, but for all Prandtl numbers larger than 0.2, the wall-mode is relevant, and the behavior of the coefficients of the amplitude equations (2) is very much like that for $\sigma=6.7$.

For all system parameters that we investigated, g_2 remains smaller than g_0 for the wall-modes, and therefore the convection occurs in two counterpropagating traveling waves, which are localized near the opposite y boundaries [1]. The coefficients of the amplitude equations for the wall-modes that are relevant for small σ and $\Omega>\Omega_{max}$, are similar to the coefficients that we find for the wall-mode for higher Prandtl numbers, in that $c_1\approx -c_3$. In the other small-σ regime where the wall-mode is relevant, i.e., $\Omega<\Omega_{min}$, there appears to be a tiny regime, close to Ω_{min}, where the coefficients c_1 and c_3 might move away from the dissipative limit; however, the numerics are not decisive here.

From the point of view of the amplitude equations, the wall-modes do not have many interesting features, and therefore we will focus now on the bulk-modes that are relevant for small Prandtl numbers and $\Omega_{min}<\Omega<\Omega_{max}$. The coefficients of the amplitude equations (2) for the bulk-mode are shown in Fig. 3 for $\sigma=0.15$. We find that the coefficients c_1 and c_3 can be tuned over a wide range by the rotation rate. For the system parameters that we consider, $g_2>g_0$ [see Fig. 3(d)] and the left- and right-traveling modes suppress each other. The convection patterns thus consist of a juxtaposition of patches of left- and right-traveling waves, and after careful adjustments one may have the convection exclusively consisting of either a left- or a right-traveling wave, which warrants a description with a single CGLE. Note that for such a single wave the value of c_2 is immaterial, since terms of the form $|A|^2B$ or $|B|^2A$ are zero.

At other values of the Prandtl number σ in the range $0.1\lesssim\sigma\lesssim 0.2$, the main effect of a change in σ is through a change in Ω_{min} and Ω_{max}; the coefficients of the amplitude equations depend of σ, but this dependence is rather weak, in the sense that Ω still makes the coefficients vary over a wide range. This is shown in Fig. 1, where the path that the coefficients trace in the parameter space of the CGLE is shown for three values of σ.

Can the interesting Prandtl number range $0.1\lesssim\sigma\lesssim 0.2$ be accessed experimentally? Compressed gases have $\sigma\gtrsim 0.7$

and typical liquids have even larger σ's, while liquid mercury and gallium have $\sigma = 0.025$ and $\sigma = 0.005$. However, Rayleigh-Bénard convection in superfluid ^{3}He-^{4}He mixtures is known to behave to a very good approximation as a convecting liquid with a Prandtl number which can be tuned continuously between 0.02 and about 1 [18]. Convection in rotating cells and flow visualization have recently become possible for such mixtures [19], and so this system provides a unique route to probe the regimes of phase-chaos and defect-chaos experimentally, and to compare to theoretical predictions [3,4]. Another possible realization of convection with $\sigma \approx 0.15$ is in certain gas mixtures, that might behave as reasonable good approximations to single component fluids [20].

In summary, we predict that Rayleigh-Bénard convection in a large rotating annulus is an attractive experimental realization of a supercritical CGLE with tunable coefficients for a number of reasons: (i) The onset of convection can occur either via a stationary or a Hopf bifurcation; in the latter case the mode can either consist of a *single* traveling bulk wave, or two counterpropagating wall-modes. The rotation rate can be adjusted to study the competition between these states, in analogy to the study of the co-dimension-2 points that occur in binary liquid convection [5]. (ii) The quasi-one-dimensional geometry of the system warrants a description in terms of one-dimensional amplitude equations, for both the intrinsic one-dimensional wall-modes and the intrinsic two-dimensional bulk-mode. (iii) The onset of convection occurs via a forward bifurcation; for backward bifurcations, like those in binary liquids, amplitude equations can at most give a qualitative description of the patterns. (iv) The underlying basic equations for this system, i.e., the Navier-Stokes equations, are considerably simpler than the basic equations for convection in liquid crystals or binary liquids. For instance, in the latter system, it is hard to decide which aspects of the experimentally observed chaos [21] can be described by the *quintic* CGLE, and which aspects are connected to physically relevant effects that are not captured in an amplitude description.

Note added. After submission of this paper, we became aware of a recent copy of unpublished work [22] in which it is predicted that Rossby waves in a rapidly rotating annulus heated from the outside also show very similar instabilities, both for comparable and for very small Prandtl numbers.

We have benefited from correspondence with R. E. Ecke, M. C. Cross, P. Kolodner, F. H. Busse, G. Ahlers, P. G. J. Lucas, and E. Knobloch.

[1] M. C. Cross and P. C. Hohenberg, Rev. Mod. Phys. **65**, 851 (1993).
[2] A. C. Newell, T. Passot, and J. Lega, Annu. Rev. Fluid Mech. **25**, 399 (1993).
[3] B. I. Shraiman, A. Pumir, W. van Saarloos, P. C. Hohenberg, H. Chaté, and M. Holen, Physica D **57** 241 (1992).
[4] T. Bohr, E. Bosch and W. van de Water, Nature (London) **372**, 48 (1994); D. A. Egolf and H. S. Greenside, Phys. Rev. Lett. **74**, 1751 (1995); H. Chaté, Nonlinearity **7**, 185 (1994).
[5] See W. Schöpf and W. Zimmerman, Phys. Rev. E **47**, 1739 (1993), and references therein.
[6] T. Leweke and M. Provensal, Phys. Rev. Lett. **72**, 3164 (1994).
[7] J. Lega, B. Janiaud, S. Jucquois, and V. Croquette, Phys. Rev. A **45**, 5596 (1992).
[8] F. Zhong, R. Ecke, and V. Steinberg, Phys. Rev. Lett. **67**, 2473 (1991); L. Ning and R. E. Ecke, Phys. Rev. E **47**, 3326 (1993); J. Herrmann and F. H. Busse, J. Fluid Mech. **225**, 183 (1993).
[9] R. E. Ecke, F. Zhong, and E. Knobloch, Europhys. Lett. **19**, 177 (1992).
[10] E. Y. Kuo and M. C. Cross, Phys. Rev. E **47**, R2245 (1993).
[11] H. F. Goldstein, E. Knobloch, I. Mercader, and M. Net, J. Fluid Mech. **248**, 583 (1993); **262**, 293 (1994).
[12] E. Knobloch, Phys. Fluids **8**, 1446 (1996).
[13] S. Chandrasekhar, *Hydrodynamic and Hydromagnetic Stability* (Clarendon Press, Oxford, 1961).
[14] T. Clune and E. Knobloch, Phys. Rev. E **47**, 2536 (1993).
[15] M. van Hecke (unpublished).
[16] It should be noted that when the critical Rayleigh numbers of, for instance, the bulk- and wall-modes become close, a description in terms of two coupled amplitude equations is no longer sufficient [1,5].
[17] E. D. Siggia and A. Zippelius, Phys. Rev. Lett. **47**, 835 (1981); M. C. Cross, Phys. Rev. A **27**, 490 (1983).
[18] G. Metcalfe and R. P. Behringer, J. Fluid Mech. **307**, 269 (1996).
[19] M. S. Thurlow, B. J. Brooks, P. G. J. Lucas, M. R. Ardron, J. K. Bhattacharjee and A. L. Woodcraft, J. Fluid Mech. **313**, 381 (1996); P. Lucas, A. Woodcraft, R. Matley, and W. Wong, Phys. World **9**, 23 (1996).
[20] G. Ahlers (private communication).
[21] P. Kolodner, J. A. Glazier, and H. Williams, Phys. Rev. Lett. **65**, 1579 (1990); J. A. Glazier, P. Kolodner, and H. Williams, J. Stat. Phys. **64**, 945 (1991).
[22] J. Herrmann and F. H. Busse (unpublished).